Effects of Two Photoreactive Spermine Analogues on Peptide Bond Formation and Their Application for Labeling Proteins in *Escherichia coli* Functional Ribosomal Complexes†

Ioannis Amarantos,‡ Maria A. Xaplanteri,‡ Theodora Choli-Papadopoulou,§ and Dimitrios L. Kalpaxis*,‡

Laboratory of Biochemistry, School of Medicine, University of Patras, GR-26500 Patras, Greece, and Laboratory of Biochemistry, School of Chemistry, University of Thessaloniki, GR-54006 Thessaloniki, Greece

Received January 3, 2001; Revised Manuscript Received March 13, 2001

ABSTRACT: The effect of two photoreactive analogues of spermine, N^1-azidobenzamidino- (ABA-) spermine and N^1-azidonitrobenzoyl- (ANB-) spermine, on ribosomal functions was studied in a cell-free system derived from *Escherichia coli*. In the dark, both analogues stimulated the binding of AcPhe-tRNA to poly(U)-programmed ribosomes, enhanced the stability of the ternary complex AcPhe-tRNA·poly(U)·ribosome (complex C), and caused stimulatory and inhibitory effects on peptidyltransferase activity. ABA-spermine exhibited more pronounced effects than ANB-spermine. Each photoprobe was covalently attached after irradiation to both ribosomal subunits and also to free rRNA isolated from 70S ribosomes. Photolabeled complex C showed a reactivity toward puromycin, similar to that exhibited by complex C reacting reversibly with photoprobes free in solution. The distribution of the incorporated radioactivity among the ribosomal components was determined under two experimental conditions, one stimulating and the other inhibiting peptidyltransferase activity. Under both conditions, ABA-spermine was the strongest cross-linker. Upon stimulatory conditions, 14% of ABA-[^{14}C]spermine cross-linked to complex C was bound to the protein fraction. The proteins primarily labeled were identified as S3, S4, L2, L3, L6, L15, L17, and L18. Upon inhibitory conditions, a higher percent of the incorporated radioactivity was found in ribosomal proteins, while the pattern of protein labeling was characterized by a remarkable decrease of cross-linked proteins L2, L3, L6, L15, L17. and L18 and by an increase of cross-linked proteins S9, S18, L1, L16, L22, L23, and L27. On the basis of these results and literature data, the involvement of spermine in the conformation and important functions of ribosomes is discussed.

Positively charged ions, including monovalent ions, divalent metal ions, and polyamines, are strictly required for efficient in vivo and in vitro protein synthesis (*1* and references cited therein). When ribosomes or their individual subunits are depleted of cations, they lose their ability to decipher rapidly and accurately the genetic code. However, it should be noticed that the structural and functional changes of ribosomes caused by polyamines are different from those induced by monovalent and divalent cations (*1*, *2*). Evidently, polyamines stimulate or inhibit preferentially the synthesis of specific proteins in vivo (*3* and references cited therein), improve the accuracy of protein synthesis (*4*), and stimulate the assembly of 30S ribosomal subunits from their constituents (*5*). Ribosomes from *Escherichia coli* contain mainly spermidine and putrescine (*6*). Nevertheless, small amounts of spermine, about 2 orders of magnitude lower than those of spermidine, can be detected in *E. coli* by more sensitive methods (*7*). Despite its low content, spermine is the most effective of the naturally occurring polyamines in *E. coli*, both in modulating the ribosomal functions and in decreasing the Mg^{2+} requirements for protein synthesis (*6*). Nevertheless, in addition to spermine, spermidine is also essential for establishing a poly(Phe) synthesizing in vitro system with a rate and accuracy close to the corresponding in vivo values (*4*). In a previous study (*8*), we approached the inhibitory and stimulatory effect of spermine in a protein synthesizing cell-free system derived from *E. coli* by evaluating the kinetic parameters of PTase. We demonstrated that spermine at 6 mM Mg^{2+} increases the extent of peptide bond formation and causes a concentration-dependent allosteric biphasic effect (nonessential activation in concert with partial noncompetitive inhibition) on PTase activity. More recently, we produced evidence that spermine at high concentrations, acting at the corner of the donor substrate, increases the interstem angle of tRNA and consequently orientates the peptidyl group of tRNA toward a less active position of the catalytic cavity (*9*). In contrast, the stimulatory effect observed at low concentrations of spermine seems to be related with the binding of spermine to ribosomes (*9*). Therefore, to elucidate the molecular mechanism of PTase stimulation by polyamines and also to interpret the effects

† This work was supported by a grant (99ED605) from the General Secretariat of Research and Technology, Ministry of Greece, and the European Social Fund.

* To whom correspondence should be addressed: tel, +3061-996124; fax, +3061-997690; e-mail, Dimkal@med.upatras.gr.

‡ University of Patras.

§ University of Thessaloniki.

10.1021/bi010010s CCC: $20.00
Published on Web 05/31/2001

of polyamines on other ribosomal functions, it is necessary to determine the ribosomal sites where polyamines bind. Furthermore, knowledge of polyamine−ribosome interactions is essential for understanding ribosome architecture, given that cations are viewed as essential structural components of the active ribosomes, similar to their RNA and protein components.

In the absence of crystallographic data for polyamine binding sites, indirect methods must be applied to obtain insight into the ribosomal sites where polyamines are specifically attached. To date, two methods have been used to map the polyamine binding sites in *E. coli* ribosomes, both employing homobifunctional cross-linkers: (a) fixation of [^{14}C]spermine to ribosomes with 1,5-difluoro-2,4-dinitrobenzene and analysis of [^{14}C]spermine distribution between rRNA and ribosomal proteins (*10*−*12*); (b) treatment of ribosomes with radioactive polyamines and dimethyl suberimidate and identification of the radiolabeled ribosomal proteins by two-dimensional gel electrophoresis and fluorography (*12*). However, the application of such approaches may lead to several artificial results. For instance, the use of a symmetrical reagent, such as 1,5-difluoro-2,4-dinitrobenzene or dimethyl suberimidate, can induce protein−protein and intra-rRNA cross-linking which may consequently lead to denaturation or aggregation. Furthermore, both reagents are amine-reactive cross-linkers, and the pattern of rRNA or ribosomal protein labeling depends on amino group availability in the vicinity of the polyamine binding site. On the other hand, the use of organic solvents (*10*) and vigorous conditions (*12*), or nonconstant ionic conditions during the original spermine binding incubation and the subsequent cross-linking step (*11*), may have an adverse effect on the ribosomal conformation and integrity. To circumvent these problems, we synthesized two photoactivatable analogues of spermine by linking an arylazido group at one of the terminal amino groups of spermine. Several tests were employed to demonstrate that both photoprobes retain almost all biochemical properties of the parent compound, spermine. Therefore, each azido analogue of spermine binds reversibly the ribosome, just as a natural polyamine would. When the analogue is bound, however, a further treatment by irradiation with mild ultraviolet light makes strong and lasting bonds between the azido group of the analogue and whatever lies nearby on the ribosome. In this report, we follow this approach in order to characterize more carefully the ribosomal proteins preferentially incorporating polyamines. Our results are discussed in view of the current advances on the localization of ribosomal proteins and on the evaluation of their biological properties.

EXPERIMENTAL PROCEDURES

Materials. Spermine tetrahydrochloride, puromycin dihydrochloride, heterogeneous tRNA from *E. coli* W, poly(U), *N*-(5-azido-2-nitrobenzoyl)-*N*-oxysuccinimide, and 4-aminobenzonitrile were obtained from Sigma-Aldrich. [^{14}C]Spermine tetrahydrochloride and L-[2,3,4,5,6-^{3}H]phenylalanine were purchased from Amersham. Cellulose nitrate filters (type HA, 24 mm diameter, 0.45 μm pore size) were from Millipore. Methyl-4-azidobenzoimidate was obtained from 4-azidobenzonitrile and methyl alcohol, essentially according to Ji (*13*).

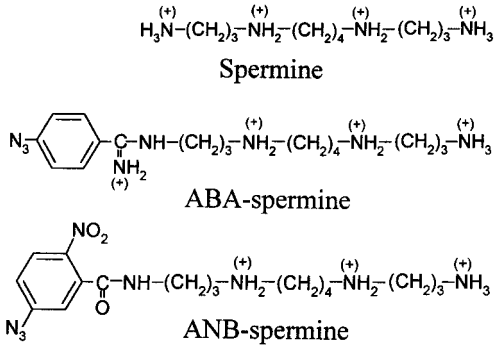

FIGURE 1: Chemical structures of spermine, ABA-spermine, and ANB-spermine. In rABA-spermine and rANB-spermine, the azido group has been replaced by an amino group.

Synthesis of Spermine Analogues. N^1-Azidonitrobenzoylspermine (ANB-spermine)[1] was synthesized from *N*-(5-azido-2-nitrobenzoyl)-*N*-oxysuccinimide and spermine and purified according to Morgan et al. (*14*). N^1-Azidobenzamidinospermine (ABA-spermine) was synthesized from methyl-4-azidobenzoimidate and spermine (*15*) and purified on a sulfopropyl-Sephadex column. ANB-spermine and ABA-spermine were converted to their reduced derivatives (rANB-spermine and rABA-spermine, respectively) with dithiothreitol according to Staros et al. (*16*). The chemical structures of spermine and its analogues are shown in Figure 1.

Biochemical Preparations. Salt-washed (0.5 M NH_4Cl) and polyamine-depleted ribosomes from *E. coli* B cells, partially purified translation factors, and crude Ac[^{3}H]Phe-tRNA charged with 15.8 pmol of [^{3}H]Phe per A_{260} unit were prepared as described elsewhere (*17*). 70S ribosomes were isolated on a 10−30% linear sucrose gradient (*18*). Native 50S and 30S ribosomal subunits were prepared by incubating 70S ribosomes in dissociation buffer (10mM Tris-HCl, pH 7.5, 0.5 mM magnesium acetate, 150 mM NH_4Cl, 6 mM 2-mercaptoethanol) at 37 °C for 15 min, followed by sedimentation in a sucrose gradient to dissociate the particles into subunits. Total rRNA was isolated from 70S ribosomes by phenol extraction and ethanol precipitation. The rRNA preparation was further purified by electrophoresis on 8% polyacrylamide/7 M urea gels, excised, and ethanol precipitated. Ribosomal proteins from 70S ribosomes (TP-70), 30S subunits (TP-30), or 50S subunits (TP-50) were isolated by precipitation with acetone from acetic acid extracts (*19*). Aliquots of ribosomal proteins (50−100 μg) were analyzed by a two-dimensional gel electrophoresis procedure developed by Brockmöller and Kamp (*20*). Initiation ribosomal complex, i.e., the Ac[^{3}H]Phe-tRNA·poly(U)·ribosome complex (complex C), was prepared and purified through adsorption on cellulose nitrate filters as described previously (*8*). The level of Ac[^{3}H]Phe-tRNA binding to poly(U)-programmed ribosomes was calculated by measuring the trapped radioactivity on the filters in a scintillation spectrometer. Controls without poly(U) were included in each experiment, and the values obtained were subtracted.

[1] Abbreviations: complex C, the Ac[^{3}H]Phe-tRNA·poly(U)·70S ribosome complex that bears Ac[^{3}H]Phe-tRNA bound at the ribosomal P site; TP-70, TP-30, and TP-50, total proteins extracted from 70S ribosomes, 30S ribosomal subunits, and 50S ribosomal subunits, respectively; PTase, ribosomal peptidyltransferase; ANB-spermine, N^1-azidonitrobenzoylspermine; ABA-spermine, N^1-azidobenzamidinospermine.

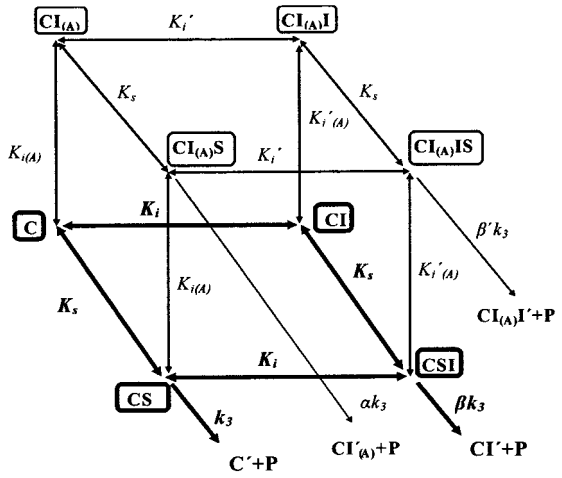

FIGURE 2: Kinetic scheme of AcPhe-puromycin synthesis carried out in a complete cell-free system derived from *E. coli* in the presence of rANB- or rABA-spermine. Abbreviations: C, complex C; S, puromycin; I and $I_{(A)}$, spermine analogue bound to the inhibition and activation site of complex C, respectively; P, AcPhe-puromycin. The region of the scheme marked in bold represents the reaction steps implicated when ribosomes are discharged from translation factors.

Peptide Bond Formation Assay. The PTase activity of ribosomes was assessed by the puromycin reaction carried out at 25 °C in the presence of 6 mM Mg^{2+} and 100 mM NH_4^+ (*21*). Under these experimental conditions, the reaction between complex C and excess puromycin (S) proceeds as an irreversible pseudo-first-order reaction to produce AcPhe-puromycin (P):

$$C + S \overset{K_s}{\rightleftharpoons} CS \overset{k_3}{\rightarrow} C' + P$$

At each concentration of puromycin, the relationship

$$k_{obs} = \frac{k_3[S]}{K_s + [S]} \quad (1)$$

holds, where k_{obs} is the first-order rate constant that can be calculated from semilogarithmic time plots (*21*), k_3 is the catalytic rate constant, and K_s is the dissociation constant of the encounter complex CS. In the presence of photoprobes (I) or whenever the puromycin reaction is carried out with photolabeled complex C, the eq 1 is converted to

$$k'_{obs} = \frac{k_{max}[S]}{K_s + [S]} \quad (2)$$

where k_{max} represents the catalytic rate constant of PTase as a function of the ligand concentration (*21*).

The values of k_3, k_{max}, and K_s were determined by linear regression of the double reciprocal plots of eq 1 or 2. To allow evaluation of the parameters employed in the kinetic scheme of Figure 2, the parameter β' was estimated directly from k'_{obs}/k_{obs} versus [I] plots and used as the fixed value in the fitting of data on appropriate theoretical equations (*21*).

Photoaffinity Labeling and Kinetics of Ligand Cross-Linking. This was carried out for ribosomal subunits or total rRNA or for complex C preparation. In the former case, ANB-[^{14}C]spermine or ABA-[^{14}C]spermine was incubated in the dark with ribosomal subunits (28.22 pmol) or total rRNA (0.4 A_{260} unit) for 10 min at 25 °C, in buffer solution (30 μL) containing 50 mM HEPES−KOH, pH 7.2, 6 mM magnesium acetate, 100 mM NH_4Cl, and 0.4 mM GTP. In the latter case, 32 A_{260} units/mL of ribosomes, 320 μg/mL poly(U), and 45 A_{260} units/mL of crude AcPhe-tRNA were added in the buffer solution. Whenever required, partially purified translation factors (400 μg/mL of protein) were also included in the above mixture. In this case, the concentration of crude AcPhe-tRNA was elevated to 65 A_{260} units/mL. The incubation mixture was then subjected to ultraviolet irradiation for specified time intervals and separated from noncovalently bound photoproducts as described previously (*9*). Nonspecific binding was measured by following the level of photoincorporation in the presence of excess spermine or reduced azido analogues. The number of cross-linking sites, the overall dissociation constant of the encounter complex between the target molecule and the photoprobe (noncovalently attached), and the Hill coefficient were estimated as indicated previously (*9*).

Cross-linked 70S ribosomes were dissociated first into ribosomal subunits and then into rRNA and ribosomal proteins. Radiolabeled proteins were identified by two-dimensional gel electrophoresis in the presence of exogenously added ribosomal proteins (*20*). Gel slabs were stained first with 0.008% Coomassie brilliant blue G-250 and then treated with 2,5-diphenyloxazole in dimethyl sulfoxide according to Bonner and Laskey (*22*). Before autoradiography, the polyacrylamide gels were soaked in a solution of 35% methanol−3.5% glycerol for 1 h and then air-dried in a cellophane sandwich (*23*). This treatment of the gels allowed them to be safely dried without distortion or cracking. The intensity of spots in autoradiograms was quantified by image analysis. The relative intensity was estimated by the formula $(A/A_o) \times 100$, where A represents the intensity of each spot and A_o the sum of intensities of all spots appearing on the autoradiogram.

RESULTS

Effects of Photoprobes on Ribosomal Functions. For application of ANB-spermine or ABA-spermine as photoprobes of the ribosome, an obligatory prerequisite is the preservation of polyamine activity after its derivatization at the N^1-position. We have previously demonstrated that spermine acylated (*21*) or alkylated (*24*) at this position is less active than the native counterpart. Therefore, the activity of photoprobes should be tested and compared to that of spermine. To avoid the irreversible attachment of photoprobes to complex C, representative experiments employing ANB-spermine or ABA-spermine were carried out in the dark. However, for practical reasons the majority of the kinetic experiments were performed in the light, using rANB-spermine or rABA-spermine as ligand. Reduced photoprobes retain fully all of the biochemical properties of photoprobes, with the exception of their azido group photoreactivity, which is nullified.

(i) Effect on the Binding of Ac[^{3}H]Phe-tRNA to Poly(U)-Programmed Ribosomes. In accordance with previous results (*21*), spermine in the absence of translation factors improves the AcPhe-tRNA binding from 3500 to about 25 000 cpm, saturating at about 200 μM (Table 1). Similarly, the binding is improved from 3500 up to a maximum of 19 000 cpm in the presence of either analogue (Table 1). When translation

Table 1: Effect of Spermine or Spermine Analogues on the AcPhe-tRNA Binding to Poly(U)-Programmed Ribosomes from *E. coli* and on the Extent of Puromycin Reaction[a]

effector	total binding/ no translation factors (cpm)	extent of puromycin reaction/ plus translation factors (%)
none	3 500	80
100 μM spermine	8 800	85
200 μM spermine	26 500	90
300 μM spermine	24 000	91
100 μM rANB-spermine	7 200	76
200 μM rANB-spermine	11 800	78
300 μM rANB-spermine	18 400	78
400 μM rANB-spermine	19 000	78
100 μM rABA-spermine	8 000	77
200 μM rABA-spermine	19 500	78
300 μM rABA-spermine	14 500	80

[a] The binding mixture (25 μL) prepared in the absence or in the presence of translation factors (10 μg of protein) contained 100 mM Tris-HCl, pH 7.2, 6 mM magnesium acetate, 100 mM NH_4Cl, 0.4 mM GTP, 320 μg/mL poly(U), 32 A_{260} units/mL of ribosomes, 13.44 A_{260} units/mL of Ac[^{3}H]Phe-tRNA, 6 mM 2-mercaptoethanol, and spermine or spermine analogues at final concentrations ranging from 100 to 400 μM. The time course of the reaction was monitored up to 30 min at 25 °C. The values of bound Ac[^{3}H]Phe-tRNA estimated by the filtration method correspond to the maximal level of binding curves.

factors are present, the stimulatory effect of spermine analogues is less pronounced (data not shown). Furthermore, rABA-spermine, in contrast to rANB-spermine, exhibits a sparing effect on Mg^{2+} requirements; addition of rABA-spermine in the binding buffer results in a lowering of the apparent Mg^{2+} optimum from 10 to about 6 mM (data not shown).

(ii) Effect on the Stability of Complex C. rANB-spermine as well as rABA-spermine enhance the stability of complex C at 6 mM Mg^{2+}, particularly of complex C formed in the absence of translation factors. For instance, when rABA-spermine concentration increases from 0 to 100 μM, the percent of complex C surviving after incubation in reaction buffer for 20 min increases from 52% to 97%. In a complete translation system, containing translation factors, complex C exhibits high stability, and therefore, the contribution of spermine analogues is marginal.

(iii) Effect on Peptide Bond Formation. When complex C is formed in the presence of translation factors, AcPhe-tRNA is translocated to the ribosomal P site. Using this well-defined complex, spermine causes only a little increase on the extent of puromycin reaction, from 80% to 90%. Both rANB-spermine and rABA-spermine keep the 80% level, although the AcPhe-tRNA binding increases from 6200 to 12 000 cpm. In the kinetic phase of the puromycin reaction and when translation factors are absent, both rANB-spermine and rABA-spermine behave as partial noncompetitive inhibitors, with one molecule of ligand involved in the mechanism of inhibition (Figure 2; bottom of the kinetic scheme, outlined by bold lines and symbols). The K_i and β values obtained by detailed kinetic analysis are summarized in Table 2. When the same experiments are carried out with complex C formed in the presence of translation factors, a distinct pattern of PTase modulation is emerging. As shown in Figure 3, concentrations up to a certain limit for each analogue stimulate PTase activity, while higher concentrations inhibit it. Kinetic analysis, similar to that applied for the interpretation of the spermine bimodal action (*21*), revealed that the overall kinetic scheme of Figure 2 is required to explain these results. The values of the kinetic parameters, obtained by nonlinear regression fitting (*21*), are presented in Table 3.

Table 2: Kinetic Parameters of AcPhe-puromycin Synthesis Carried Out in the Presence of Spermine or Spermine Analogues with Complex C Formed in the Absence of Translation Factors[a]

effector	K_i (μM)	β
spermine	120 ± 8	0.160 ± 0.010
rANB-spermine	268 ± 15	0.107 ± 0.007
rABA-spermine	297 ± 13	0.357 ± 0.018

[a] The reaction was carried out in buffer containing 6 mM Mg^{2+}, 100 mM NH_4^+, and spermine or spermine analogues at final concentrations ranging from 0 to 0.8 mM. The K_s and k_3 values estimated by linear regression of the double reciprocal plot of eq 1 are 665 ± 37 μM and 1.4 ± 0.1 min^{-1}, respectively.

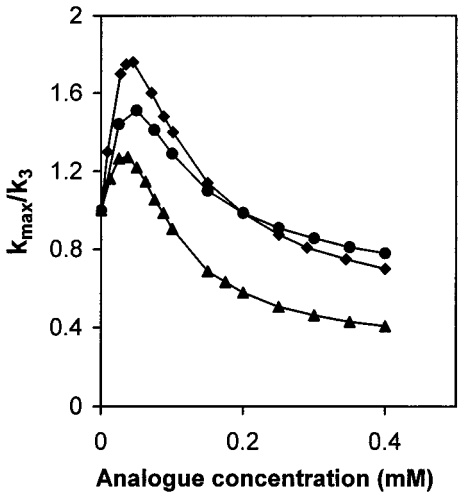

FIGURE 3: Variation of k_{max}/k_3 as a function of spermine analogue concentration. Complex C formed in the presence of translation factors reacted with puromycin in buffer containing 6 mM Mg^{2+}, 100 mM NH_4^+, and spermine (◆), rANB-spermine (▲), or rABA-spermine (●) at the indicated concentrations. The k_{max} values were estimated from the corresponding double reciprocal plots of eq 2 by linear regression. Similarly, the k_3 and K_s values were calculated by using eq 1 and were found equal to 2.22 ± 0.05 min^{-1} and 665 ± 35 μM, respectively.

Table 3: Kinetic Parameters of AcPhe-puromycin Synthesis Carried Out in the Presence of Spermine or Spermine Analogues with Complex C Formed in the Presence of Translation Factors[a]

effector	$[I]_{opt}$ (μM)	$K_{i(A)}$ (mM)	K_I' (μM)	α	β'	relative activity of PTase (%)[b]
control						100
spermine	50	3.20	0.80	149.8	0.450	175
rANB-spermine	40	1.53	2.60	16.2	0.265	128
rABA-spermine	50	0.95	3.40	28.7	0.550	151

[a] The reaction was carried out in buffer containing 6 mM Mg^{2+}, 100 mM NH_4^+, and spermine or spermine analogues at final concentrations ranging from 0 to 0.4 mM. The K_s and k_3 values estimated by linear regression of the double reciprocal plot of eq 1 are 665 ± 35 μM and 2.22 ± 0.05 min^{-1}. [b] The relative activity of PTase estimated from the maximum level of the curves presented in Figure 3 is expressed as a percentage of the control value ($k_{max}/k_3 \times 100$).

Cross-Linking of Photoprobes to Ribosomal Complex C, Ribosomal Subunits, or rRNA. Under appropriate irradiation, the arylazido group of ANB-spermine or ABA-spermine is converted to nitrene, a highly reactive species which is able

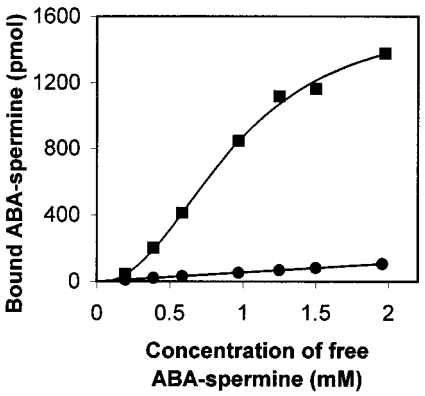

FIGURE 4: ABA-spermine photoincorporation into 50S ribosomal subunits at various concentrations of photoprobe. The photoaffinity labeling was carried out in buffer solution (30 μL) containing 50 mM HEPES−HCl, pH 7.2, 6 mM magnesium acetate, 100 mM NH_4Cl, 0.4 mM GTP, and 28.22 pmol of 50S ribosomal subunits. Symbols: (■) specific binding; (●) nonspecific binding estimated by measuring the photoincorporation in the simultaneous presence of excess spermine.

Table 4: Hill Plot Analysis of ANB-spermine or ABA-spermine Photoincorporation to Ribosomal Subunits or Ribosomal RNA[a]

target molecule	N	K_D (mM^n)	n
(a) Photolabeling with ANB-spermine			
30S ribosomal subunits	248 ± 15	1.62 ± 0.18	1.85 ± 0.39
50S ribosomal subunits	301 ± 10	3.86 ± 0.71	2.30 ± 0.65
total rRNA	29 ± 3	0.35 ± 0.09	1.80 ± 0.24
(b) Photolabeling with ABA-spermine			
30S ribosomal subunits	39.3 ± 2.2	0.84 ± 0.11	2.02 ± 0.30
50S ribosomal subunits	57.4 ± 1.1	0.86 ± 0.04	2.30 ± 0.37
total rRNA	20.6 ± 3.5	0.13 ± 0.07	2.00 ± 0.74

[a] The photoaffinity labeling of ribosomal subunits (28.22 pmol) or total rRNA (0.2 A_{260} unit) was carried out in buffer solution (30 μL) containing 50 mM HEPES−HCl, pH 7.2, 6 mM Mg^{2+}, 100 mM NH_4^+, 0.4 mM GTP, and ANB-[^{14}C]spermine or ABA-[^{14}C]spermine at final concentrations ranging from 0.05 to 2 mM. N, K_D, and n represent the number of binding sites under saturation conditions, the overall dissociation constant, and the Hill coefficient, respectively.

to react with a variety of adjacent groups of the target molecule (*14*). Control experiments showed that ribosomes or ribosomal subunits are not inactivated upon irradiation in the absence of photoprobes. Photolabeling data at various concentrations of ANB-spermine or ABA-spermine establish for each one of the target molecules a sigmoidal hyperbola, such as the one shown in Figure 4. Therefore, the data are fitted to eq 3 by the Hill hyperbola function of the Microcal

$$B = \frac{B_{max}[F]^n}{K_D + [F]^n} \quad (3)$$

Origin 4.00 program (Microcal Software, Inc.). In eq 3, [F] is the concentration of free photoprobe, B_{max} is the maximum level of covalently linked photoprobe, and K_D is the overall dissociation constant of the encounter complex between the target molecule and the photoprobe. The results obtained by this analysis are summarized in Table 4.

Activity of Photolabeled Ribosomal Complexes and Distribution of the Cross-Linked Spermine within Ribosomal Complexes at Different Phases of PTase Modulation. Photoincorporation of ANB-spermine or ABA-spermine into complex C modulates the PTase activity in a manner dependent on the experimental conditions under which complex C is formed (*9*). To investigate this effect in detail, several ribosomal complexes photolabeled at various concentrations of photoprobes were constructed, and their activity in catalyzing peptide bond formation was titrated with puromycin. The results found are reminiscent of those obtained with rABA-spermine or rANB-spermine reacting in solution (reversible interaction). Taking this into account, we decided to analyze the cross-linking of spermine to complex C under two different experimental conditions: (a) when complex C is formed in the absence of translation factors and photolabeled at 300 μM of photoprobe (condition A); (b) when complex C is formed in the presence of translation factors and photolabeled at 50 μM (condition B). It was found that 26% of ribosomes prepared under condition A and 20% of ribosomes prepared under condition B are charged with AcPhe-tRNA. Following removal of free ribosomal subunits by sucrose gradient centrifugation, the percent of active ribosomes in AcPhe-tRNA binding is elevated to 94% and 37%, respectively. Under condition A, ANB-spermine and ABA-spermine become cross-linked to complex C in a yield of 15.6% and 17%, respectively. Also, a 38.1% and 29.3% inhibition of PTase activity is attained in the case of photolabeling with 300 μM ANB-spermine and ABA-spermine, respectively. These values agree well with a 47% and 33.9% inhibition caused by 300 μM rANB-spermine and rABA-spermine, respectively. Under condition B, ANB-spermine and ABA-spermine are cross-linked to complex C in a yield of 1.4% and 0.7%, respectively. In this case, the attachment of ANB-spermine and ABA-spermine to ribosomes increases the reactivity of complex C toward puromycin by causing a 36.8% and 55.8% stimulation of PTase activity, respectively. These properties are reminiscent of the behavior of rANB-spermine and rABA-spermine, which under the same experimental conditions cause a 27.6% and 51% stimulation, respectively (Table 3).

A representative sucrose gradient analysis of radiolabeled ribosomes with ABA-spermine is shown in Figure 5. Nearly similar results are obtained, using ANB-spermine instead of ABA-spermine. 50S and 30S peaks, detected under association conditions (see Materials and Methods), represent free ribosomal subunits preexisting in the initial ribosomal population. While under condition B the major species of ribosomes are 70S monomers (Figure 5, panel A), in the absence of translation factors (condition A) the level of 70S particles decreases (Figure 5, panel B), reaching about 27% of total ribosomes. It is evident that the specific radioactivity (cpm/A_{260}) of free 30S subunits is higher than that of 70S or 50S particles under both experimental conditions. However, there is no detectable difference in sedimentation between natural and photolabeled ribosomal particles. Subsequent centrifugation of 70S ribosomes in gradients containing low Mg^{2+} concentrations (Figure 5, panels C and D) dissociates them into 50S and 30S subunits. To determine the distribution of the cross-linked photoprobes within ribosomal subunits, protein and RNA components are separated and counted for radioactivity. As indicated in Table 5, rRNA is labeled to a higher extent than ribosomal proteins.

Ribosomal Proteins Labeled by ANB-spermine or ABA-spermine. The results obtained by two-dimensional gel electrophoresis of 50S and 30S ribosomal proteins, followed by autoradiography and image analysis of the individual

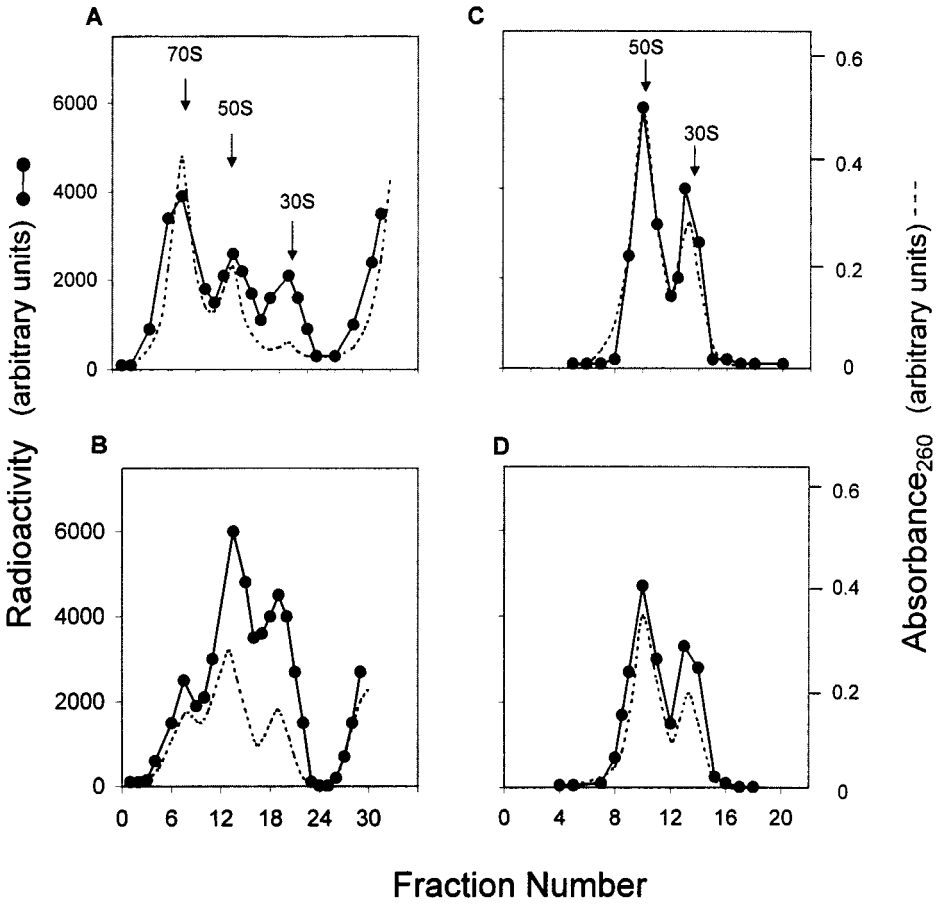

FIGURE 5: Sucrose gradient analysis of the products of ABA-spermine cross-linking to complex C. Panels A and B are of ribosomal complexes photolabeled with ABA-spermine under stimulatory and inhibitory conditions, respectively. In both cases, the product of cross-linking was sedimented through 10−30% gradients of sucrose in buffer containing 10 mM Tris-HCl, pH 7.5, 6 mM $MgCl_2$, 30 mM NH_4Cl, and 6 mM β-mercaptoethanol. The gradients were calibrated with 70S ribosomes and with 50S and 30S ribosomal subunits isolated from *E. coli* B cells. After centrifugation, the gradients were processed for optical scanning at 260 nm (⋯) and radioactivity counting (●). Panels C and D give the corresponding gradients of samples obtained from the 70S area of gradients such as shown in panels A and B, respectively, after incubation and centrifugation under dissociation conditions (0.5 mM Mg^{2+}, 150 mM NH_4^+). The amount of radioactivity and absorbance at 260 nm are indicated in arbitrary units to allow a direct comparison of the individual profiles.

protein spots, are summarized in Table 5. Representative autoradiograms are shown in Figure 6. Proteins cross-linked to ANB-spermine or ABA-spermine appear at positions slightly more basic than those of natural proteins. ANB-spermine interacts primarily with proteins of the 30S subunit (S3, S4, S7), while four proteins (namely, L2, L3, L4, and L6) of the 50S subunit are also labeled in a lower yield. In contrast, ABA-spermine labels numerous proteins in both ribosomal subunits. These proteins could be divided into two groups, the first of which contains the more strongly labeled proteins S3, S4, S5, L2, L3, L6, L10, L15, L17, L18, L19, L22, and L27, under certain conditions. The second group includes proteins S2, S6, S7, S9, S16, S17, L1, L4, L16, and L23, which show less but still measurable amounts of radioactivity. Some other proteins give only faint spots (Table 5). Ribosomal proteins in free subunits appear to be more susceptible to cross-linking than proteins in complex C (Table 5). Also, the pattern of labeled proteins seems to depend on the experimental conditions (A or B) followed during photolabeling (Table 5). As a control, free ribosomal proteins are treated essentially under the same conditions as above. The radioactivity measured in these proteins is about one-half the radioactivity incorporated in proteins extracted from an equivalent amount of labeled ribosomal subunits or complex C. Moreover, the pattern of radioactivity distribution among these proteins differs. Such a comparative analysis is given in Figure 7, concerning proteins of the small ribosomal subunit.

DISCUSSION

Numerous studies have demonstrated that the maintainance of the structural and functional integrity of ribosomes depends on the establishment of an environment of thermodynamically bound ions, such as polyamines and monovalent and divalent ions (*1* and references cited therein, *25*, *26*). Since the beginning of these studies, it was well understood that mapping the ion binding sites in ribosomes could facilitate the investigation of their mode of action. Therefore, several studies have been focused on polyamine (*10*−*12*) or metal ion (*27* and references cited therein) probing of ribosomes. Recently, we mapped the cross-linking sites of ANB-spermine and ABA-spermine in AcPhe-tRNA bound at the P site of *E. coli* ribosomes (*9*). The use of these analogues for mapping polyamine binding sites has several advantages compared to other approaches (*10*−*12*). The azido group can easily react through irradiation with a variety of adjacent groups in proteins or RNA. Thus, attachment of ANB-spermine or ABA-spermine does not depend on

Table 5: Ribosomal Proteins Radioactively Labeled with ANB-[^{14}C]spermine or ABA-[^{14}C]spermine and Distribution of Labeling between Ribosomal Proteins and rRNA

target molecule	exptl conditions[a]	% distribution TP-30/ 16S rRNA	% distribution TP-50/ 23S + 5S rRNA	labeled proteins[b]
(a) Photolabeling with ANB-[^{14}C]spermine				
complex C	A	6.5:93.5	6.8:93.2	**S3**, **S4**, **L2**, L3, (L4), L6
	B	4.0:96.0	3.5:96.5	**S4**, (L2), (L3)
30S ribosomal subunits	A	11.6:88.4		S3, **S4**, S7
	B	5.8:94.2		**S4**
50S ribosomal subunits	A		13.5:86.5	L2, L3, (L4), L6
	B		7.1:92.3	L2, (L3)
(b) Photolabeling with ABA-[^{14}C]spermine				
complex C	A	25.2:74.8	26.2:73.8	S2, **S3**, **S4**, **S5** (S6), S9, S16, S17, (S18), L1, L2, L3, L4, L6, (L13), L15, L16, L17, L18, **L19**, **L22**, L23, (L24), **L27**
	B	14.2:85.8	13.7:86.3	(S2), **S3**, **S4**, S5, (S6), (S9), S16, S17, (L1), **L2**, **L3**, L4, **L6**, (L13), **L15**, (L16), **L17**, **L18**, (L19), (L22), (L23), (L24), (L27)
30S ribosomal subunits	A	24.6:75.4		S2, **S3**, **S4**, **S5**, S6, S7, S9, (S13), (S14), S16, S17, (S18)
	B	14.2:85.8		S2, **S3**, **S4**, S5, (S6), S7, S9, S16, S17
50S ribosomal subunits	A		43.1:56.9	(L1), L2, L3, (L4), (L5), L6, (L9), **L10**, L15, (L16), L17, L18, **L19**, **L22**, (L23), L27
	B		20.5:79.5	(L1), **L2**, **L3**, (L4), **L6**, L10, L15, (L16), **L17**, **L18**, (L19), (L22), (L23), (L27)

[a] The target molecule was formed (A) in the absence of translation factors and labeled at high concentration of photoprobe (300 μM) or (B) in the presence of translation factors and photolabeled at low concentration of photoprobe (50 μM). At both conditions, the concentration of Mg^{2+} and NH_4^+ ions was 6 and 100 mM, respectively. [b] Ribosomal proteins highly labeled are indicated by bold symbols, while proteins weakly labeled are enclosed in parentheses.

fortuitous juxtaposition of specific groups, capable of reacting with the cross-linking agent. Moreover, the arylazido tether of ANB-spermine or ABA-spermine is about 8 and 9 Å in length, respectively. This level of resolution is sufficient for ribosomes, which have overall dimensions of about 250 Å. In addition, the photolabeling procedure that we apply does not require vigorous conditions that may destroy the ribosomal conformation and does not induce protein−protein cross-linking which may lead to loss or ambiguities in protein identification. However, more important of all is the preservation of polyamine biological properties in photoprobes, despite the derivatization of spermine at one of its terminal amino groups. This rule is better followed by ABA-spermine, which retains a charge in the vicinity of the nearest amino group. Nevertheless, the arylazido substituent of spermine may compromise some electrostatic interactions by increasing the distance between the analogue and the inhibition site of complex C. As a consequence, the ability of each analogue to interact with complex C is decreased (increased K_i values, Table 2). rABA-spermine behaves as a weaker inhibitor, since its high β value increases the reactivity of the corresponding CIS complex (Figure 2). This is also confirmed by the high $K_i'$and β' values determined in a complete translation system containing translation factors (Table 3). However, in the presence of translation factors a specific conformation is conferred to complex C, so that the ribosomal complex is rearranged to accommodate a second ligand binding site with activatory properties (Figure 2). The affinity of rABA-spermine for the activation site as well as the reactivity of $CI_{(A)}S$ complex are higher (lower $K_{I(A)}$ value, higher α value) compared to those of rANB-spermine (Table 3). Therefore, the PTase activation by rABA-spermine approximates better the stimulation level obtained by spermine (Figure 3).

Although the kinetic analysis of puromycin reaction reveals two binding sites in maximum, a higher number of photoprobe molecules have been found to be incorporated by irradiation into complex C (*9*). We assume that these additional molecules are not involved kinetically in the mechanism of PTase regulation but probably confer a specific conformation to complex C, which may play an important role in other ribosomal functions. In photolabeling experiments, the affinity of ABA-spermine for each of the target molecules seems to be higher than that of ANB-spermine (Table 4). On the other hand, naked rRNA behaves as the stronger acceptor of photoprobes, as shown by its low K_D (Table 4). In contrast, Bernabeu et al. (*11*) and Kakegawa et al. (*12*) failed to cross-link spermine to free rRNA. This can be attributed to the low cross-linking reactivity of the reagents used in these studies toward RNA. Interestingly, complex C photolabeled and discharged from noncovalently bound photoprobes exhibits similar reactivity toward puromycin, compared to complex C interacting reversibly with the same amount of photoprobes in solution. This finding further supports the specificity of photoprobe attachment to the target molecule and reveals another advantage of our experimental approach.

Comparing the results shown in Table 4 with those obtained in a previous study (*9*), it becomes clear that free ribosomal subunits, in particular 30S subunits, are more susceptible to photoprobe cross-linking than 70S ribosomes. This was confirmed by sucrose gradient analysis (Figure 5), and it is in agreement with observations made by Bernabeu et al. (*11*). The radioactivity incorporated into 70S ribosomes is equally distributed (cpm/A_{260}) between 30S and 50S subunits. However, rRNA is labeled to a higher extent than ribosomal proteins (Table 5). The yield of photoprobe cross-linking and the distribution of incorporated radioactivity are similar to those obtained by a previous study using dimethyl suberimidate as cross-linking reagent (*12*) but differ from those reported in other studies using 1,5-difluoro-2,4-dinitrobenzene (*10*, *11*).

The number and the intensity of autoradiography spots corresponding to labeled proteins by ANB-spermine are

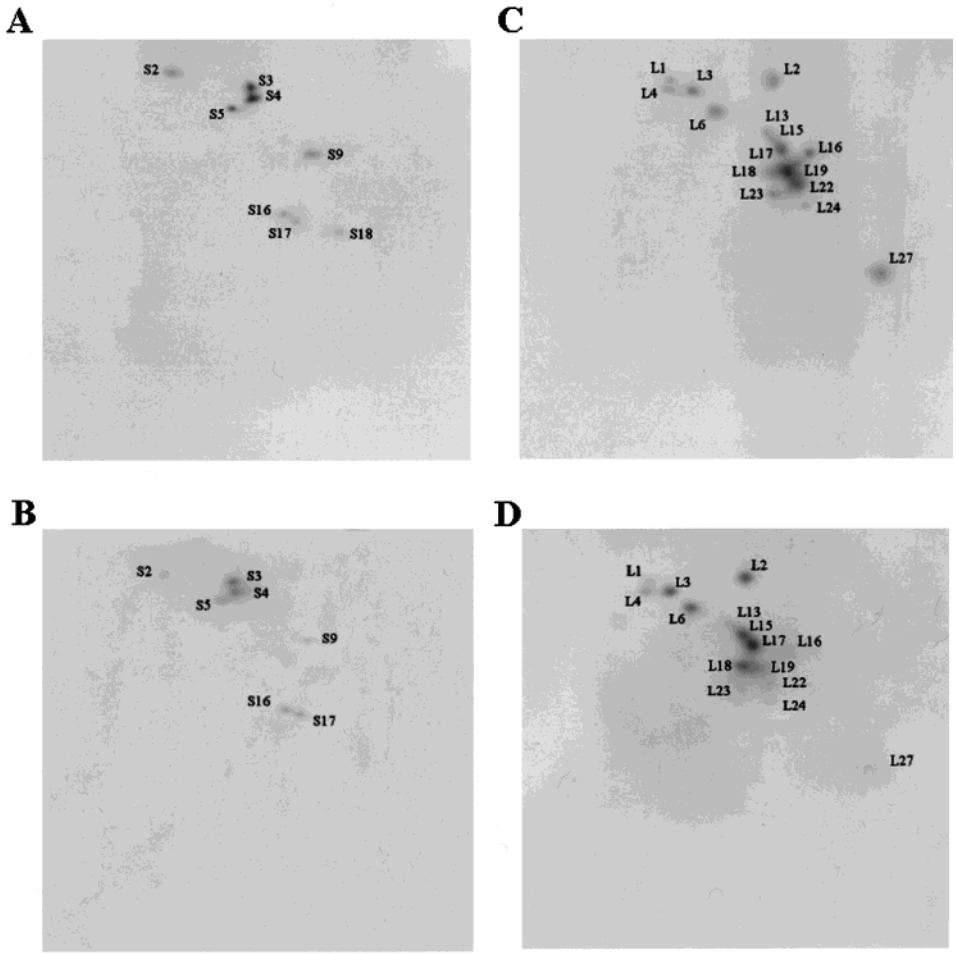

FIGURE 6: Electrophoretic analysis of proteins cross-linked to ABA-spermine. The gel system is that of Brockmöller and Kamp (*20*), with the direction of electrophoresis being from left to right (first dimension) and top to botttom (second dimension). Panels A and C: TP-30 and TP-50 radiolabeled proteins, respectively, isolated from complex C treated under condition A. Panels B and D: TP-30 and TP-50 radiolabeled proteins, respectively, isolated from complex C treated under condition B.

significantly lower than those observed in photolabeling using ABA-spermine (Table 5). This may be explained by the fact that a higher percentage of radioactivity is distributed to proteins when ABA-[^{14}C]spermine is used as photoprobe. As a consequence, ABA-spermine binds a number of proteins additional to those labeled by ANB-spermine, some of which (S6, S13, S16, S17, L4, L10, L15, L23) were not detected in previous studies (*11*, *12*). In general, the species of proteins labeled by ABA-spermine in free ribosomal subunits do not significantly differ from those detected in 70S ribosomes. However, a closer view shows that six interface proteins (*28*−*31*), namely, S6, S7, S13, S14, L5, and L10, are labeled when ribosomal subunits, not 70S ribosomes, are used. Probably, association of ribosomal subunits lowers the accessibility of these proteins to the photoprobe. Also, the spot of L9 is missing when 70S ribosomes instead of 50S subunits are examined. This is consistent with the cryoelectron microscopy finding (*32*) that protein L9 appears to move from its solvent-exposed position in free 50S subunits to the 30S−50S interface area within the 70S complex, enveloped in structural elements arising from the small subunit. A quantitative change occurring in 50S subunit labeling upon 30S subunit association is the enhancement of intensity of the spots corresponding to proteins L2, L3, L4, L6, L13, and L15. It is known that these proteins interact with domain V, despite the fact that there are no globular proteins in the vicinity of the PTase center (*33*). Nevertheless, nonglobular extensions of L2, L3, and L4 slip deeply into the PTase cleft (*33*). Cryoelectron microscopy studies (*32*) as well as protection experiments (*34*) have demonstrated a sharp PTase cleft opening upon subunit association. Therefore, it is tempting to suggest that the high accessibility of L2, L3, L4, L6, L13, and L15 proteins to ABA-spermine in 70S ribosomes is related to the above conformational change.

By comparing the pattern of radioactive ribosomal 30S proteins obtained from labeling 70S ribosomes under condition A to that obtained under condition B, it is clear that in general the two patterns resemble each other. The exceptions are S9 and S18, for which the two patterns differ. Protein S9 participates in intersubunit RNA−protein contacts (*35*), clustered on the small protuberance of the 50S subunit and on the platform of the 30S subunit. The labeling of S9 to a greater extent under condition A probably indicates a loosening of intersubunit contacts, conjugated with functional alterations of the ribosomal complex. Although protein S18 is implicated in intersubunit connection (*32*), an interpretation of its deviated behavior on the same basis has to be regarded with caution. Protein S18 is a highly reactive protein often giving several nonspecific affinity labels (*36*), in particular whenever the concentration of photoprobe is raised. S3, S4, and S5 are the most strongly cross-linked proteins in the small subunit, independently of whether photolabeling of

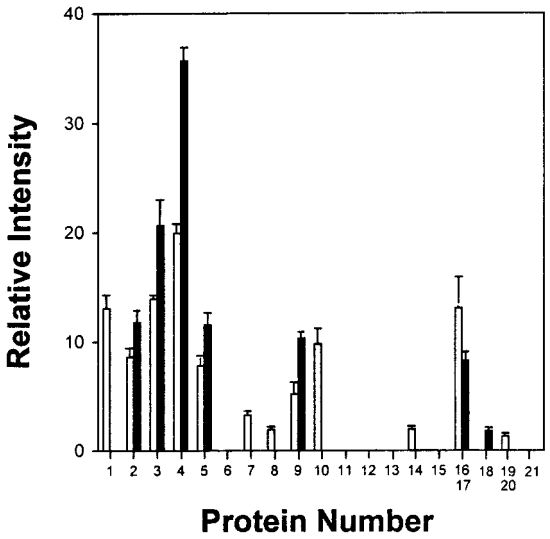

FIGURE 7: Histogram presenting the relative intensity of radiolabeled spots quantified by image analysis. The solid bars correspond to TP-30 proteins extracted from complex C labeled under condition A, while the open bars correspond to TP-30 free proteins labeled under the same condition. The relative intensity was estimated by the formula $(A/A_o) \times 100$, where A represents the intensity of each spot and A_o the sum of intensities of all spots appearing on the autoradiogram.

complex C preparation is carried out under condition A or B. These proteins are not involved directly in PTase activity but are implicated in various ribosomal functions, most notably aminoacyl-tRNA binding to ribosomes (S3, S4, S5), ribosomal accuracy (S4, S5), translocation (S3, S4, S5), and peptide chain termination (S4, S5). As reviewed by Cohen (*37*), all of these functions are regulated by polyamines.

No differences in the diversity of cross-linked proteins from the large ribosomal subunit are observed when complex C is photolabeled under condition A or B. However, remarkable differences in the extent of photolabeling for each protein are visible, which may help to gain insight into the mechanism of spermine action on PTase activity. Upon conditions promoting high activity in PTase, the most strongly labeled species (L2, L3, L6, L15, L17, L18) are proteins topographically adjacent to the PTase center (*33*, *36*, *38*−*41*). Under inhibitory conditions, the bulk of labeling shifts from the above proteins to proteins L1, L16, L19, L22, L23, and L27, which are positioned less adjacently to the PTase center. This shift suggests that a preferential attachment of polyamines to specific "PTase proteins" has a beneficial effect on the catalytic properties of ribosomal complex C. Definitive elucidation of important details of this mechanism remains elusive. Bound polyamines possibly influence the conformation of specific "PTase proteins", which in turn may affect the conformation of ribosomal RNA residues possessed of catalytic power. However, it cannot be excluded that polyamine binding to ribosomal proteins neighboring the PTase center may provide the active center with an amino group bearing a near neutral pK_a that serves as a stabilizer of intermediates or as a general acid/base during peptide bond formation (*33*, *42*). Given that activation of PTase does not occur in the absence of translation factors, we assume that some type of structural reorganization of ribosomes due to the actions of these factors is important in rendering specific ribosomal proteins recognizable by polyamines.

The cross-linking of photoprobes to specific ribosomal proteins could be due simply to the intrinsic chemical reactivity of these proteins toward polyamine. Alternatively, spermine may originally bind to rRNA, and while attached there it may cross-link with adjacent ribosomal proteins, as has been suggested by previous studies (*10*−*12*). An indication that such a mechanism may exists comes from our finding that free ribosomal proteins and ribosomal subunits or complex C differ with respect to the yield and pattern of photolabeling. To date, there have been no studies on the cross-linking sites of spermine with rRNA, and for this reason current work in our laboratory has been focused on this subject.

ACKNOWLEDGMENT

We thank Denis Drainas and Dennis Synetos for critical reading of the manuscript.

REFERENCES

1. Michelinaki, M., Spanos, A., Coutsogeorgopoulos, C., and Kalpaxis, D. L. (1997) *Biochim. Biophys. Acta 1342*, 182−190.
2. Igarashi, K., and Kashiwagi, K. (2000) *Biochem. Biophys. Res. Commun. 271*, 559−564.
3. Igarashi, K., Saisho, T., Yuguchi, M., and Kashiwagi, K. (1997) *J. Biol. Chem. 272*, 4058−4064.
4. Bartetzko, A., and Nierhaus, K. H. (1988) *Methods Enzymol. 164*, 650−658.
5. Kakegawa, T., Hirose, S., Kashiwagi, K., and Igarashi, K. (1986) *Eur. J. Biochem. 158*, 265−269.
6. Tabor, C. W., and Tabor, H. (1976) *Annu. Rev. Biochem. 45*, 285−306.
7. Kamekura, M., Hamana, K., and Matsuzaki, S. (1987) *FEMS Microbiol. Lett. 43*, 301−305.
8. Drainas, D., and Kalpaxis, D. L. (1994) *Biochim. Biophys. Acta 1208*, 55−64.
9. Amarantos, I., and Kalpaxis, D. L. (2000) *Nucleic Acids Res. 28*, 3733−3742.
10. Stevens, L., and Pascoe, G. (1972) *Biochem. J. 128*, 279−289.
11. Bernabeu, C., Vazques, D., and Ballesta, J. P. G. (1978) *Biochim. Biophys. Acta 518*, 290−297.
12. Kakegawa, T., Sato, E., Hirose, S., and Igarashi, K. (1986) *Arch. Biochem. Biophys. 251*, 413−420.
13. Ji, T. H. (1977) *J. Biol. Chem. 252*, 1566−1570.
14. Morgan, J. E., Calkins, C. C., and Matthews, H. R. (1989) *Biochemistry 28*, 5095−5106.
15. Clark, E., Swank, R. A., Morgan, J. E., Basu, H., and Matthews, H. R. (1991) *Biochemistry 30*, 4009−4020.
16. Staros, J. V., Bayley, H., Standring, D. N., and Knowles, J. R. (1978) *Biochem. Biophys. Res. Commun. 80*, 568−572.
17. Kalpaxis, D. L., Theocharis, D., and Coutsogeorgopoulos, C. (1986*) Eur. J. Biochem. 154*, 267−271.
18. Kalpaxis, D. L., Karahalios, P., and Papapetropoulou, M. (1998) *J. Bacteriol. 180*, 3114−3119.
19. Barritault, D., Expert-Benzacon, A., Guerin, M. F., and Hayes, D. (1976) *Eur. J. Biochem. 63*, 131−135.
20. Brockmöller, H.-J., and Kamp, R. M. (1986) in *Advanced Methods in Protein Microsequence Analysis* (Wittmann-Liebold, B., Salnikow, J., and Erdmann, V. A., Eds.) pp 34−44, Springer-Verlag, Berlin.
21. Karahalios, P., Mamos, P., Karigiannis, G., and Kalpaxis, D. L. (1998) *Eur. J. Biochem. 258*, 437−444.
22. Bonner, W. M., and Laskey, R. A. (1974) *Eur. J. Biochem. 46*, 83−88.
23. Michaels, S. D., and Ford, J. C. (1991) *BioTechniques 11*, 466−467.
24. Karahalios, P., Amarantos, I., Mamos, P., Papaioannou, D., and Kalpaxis, D. L. (1999) *J. Bacteriol. 181*, 3904−3911.

25. Batey, R. T., and Williamson, J. R. (1998) *RNA 4*, 984−997.
26. Noah, J. W., and Wollenzien, P. (1998) *Biochemistry 37*, 15442−15448.
27. Polacek, N., and Barta, A. (1998) *RNA 4*, 1282−1294.
28. Clemons, W. M., May, J. L. C., Wimberly, B. T., McCutcheon, J. P., Capel, M. S., and Ramakrishnan, V. (1999) *Nature 400*, 833−840.
29. Schluenzen, F., Tocilj, A., Zarivach, R., Harms, J., Gluehmann, M., Janell, D., Bashan, A., Bartels, H., Agmon, I., Franceschi, F., and Yonath, A. (2000) *Cell 102*, 615−623.
30. Ban, N., Nissen, P., Hansen, J., Moore, P. B., and Steitz, T. A. (2000) *Science 289*, 905−920.
31. Gabashvili, I. S., Agrawal, R. K., Spahn, C. M., Grassucci, R. A., Svergun, D. I., Frank, J., and Penczek, P. (2000*) Cell 100*, 537−549.
32. Matadeen, R., Patwardhan, A., Gowen, B., Orlova, E. V., Pape, T., Cuff, M., Mueller, F., Brimacombe, R., and van Heel, M. (1999) *Struct. Folding Des. 7*, 1575−1583.
33. Nissen, P., Hansen, J., Ban, N., Moore, P. B., and Steitz, T. A. (2000) *Science 289*, 920−930.
34. Merryman, C., Moazed, D., Daubresse, G., and Noller, H. F. (1999) *J. Mol. Biol. 285*, 107−113.
35. Abdurashidova, G. G., Tsvetkova, E. A., Chernyi, A. A., Kaminir, L. B., and Budowsky, E. I. (1985) *FEBS Lett. 185*, 291−294.
36. Nicholson, A. W., Hall, C. C., Strycharz, W. A., and Cooperman, B. S. (1982) *Biochemistry 21*, 3797−3808.
37. Cohen, S. S. (1998) in *A Guide to the Polyamines*, pp 512−543, Oxford University Press, New York.
38. Hampl, H., Schulze, H., and Nierhaus, K. H. (1981) *J. Biol. Chem. 256*, 2284−2288.
39. Traut, R. R., Tewari, D. S., Sommer, A., Gavino, G. R., Olson, H. M., and Glitz, D. (1986) in *Structure, Function and Genetics of Ribosomes* (Hardesty, B., and Kramer, G., Eds.) pp 286−308, Springer-Verlag, Berlin.
40. Cooperman, B. S., Weitzman, C. J., and Fernandez, C. L. (1990) in *The Ribosome Structure Function and Evolution* (Hill, W. E., Dahlerg, A., Garrett, R. A., Moore, P. B., Schlessinger, D., and Werner, J. S., Eds.) pp 123−133, American Society for Microbiology, Washington, DC.
41. Bischof, O., Urlaub, H., Kruft, V., and Wittmann-Liebold, B. (1995) *J. Biol. Chem. 270*, 23060−23064.
42. Muth, G. W., Ortoleva-Donnelly, L., and Strobel, S. A. (2000) *Science 289*, 947−950.

BI010010S